Diabetes 2009

Dataset · July 2014

5 authors, including:

U Rajendra Acharya
Ngee Ann Polytechnic, SIM University, SIT-…
424 PUBLICATIONS **7,617** CITATIONS
SEE PROFILE

Choo Min Lim
Ngee Ann Polytechnic
152 PUBLICATIONS **3,549** CITATIONS
SEE PROFILE

Eddie YK Ng
Nanyang Technological University
372 PUBLICATIONS **4,305** CITATIONS
SEE PROFILE

Toshiyo Tamura
Waseda University
320 PUBLICATIONS **2,432** CITATIONS
SEE PROFILE

Computer-based detection of diabetes retinopathy stages using digital fundus images

U R Acharya[1*], **C M Lim**[1], **E Y K Ng**[2], **C Chee**[3], and **T Tamura**[4]
[1]Department of Electronics and Computer Engineering, Ngee Ann Polytechnic, Singapore
[2]School of Mechanical and Aerospace Engineering, College of Engineering, Nanyang Technological University, Singapore
[3]NUH Eye Surgery, Department of Opthalmology, National University Hospital, Singapore
[4]Department of Medical System Engineering, Chiba University, Japan

The manuscript was received on 31 July 2008 and was accepted after revision for publication on 6 February 2009.

DOI: 10.1243/09544119JEIM486

Abstract: Diabetes mellitus is a heterogeneous clinical syndrome characterized by hyperglycaemia and the long-term complications are retinopathy, neuropathy, nephropathy, and cardiomyopathy. It is a leading cause of blindness. Diabetic retinopathy is the progressive pathological alterations in the retinal microvasculature, leading to areas of retinal non-perfusion, increased vascular permeability, and the pathological proliferation of retinal vessels. Hence, it is beneficial to have regular cost-effective eye screening for diabetes subjects. Nowadays, different stages of diabetes retinopathy are detected by retinal examination using indirect biomicroscopy by senior ophthalmologists. In this work, morphological image processing and support vector machine (SVM) techniques were used for the automatic diagnosis of eye health. In this study, 331 fundus images were analysed. Five groups were identified: normal retina, mild non-proliferative diabetic retinopathy, moderate non-proliferative diabetic retinopathy, severe non-proliferative diabetic retinopathy, and proliferative diabetic retinopathy. Four salient features blood vessels, microaneurysms, exudates, and haemorrhages were extracted from the raw images using image-processing techniques and fed to the SVM for classification. A sensitivity of more than 82 per cent and specificity of 86 per cent was demonstrated for the system developed.

Keywords: image, diabetes, retinopathy, morphology, support vector machine, eye, microaneurysms, exudates, haemorrhages

1 INTRODUCTION

Diabetes is the chronic state caused by an abnormal increase in the glucose level in the blood and which causes the damage to the blood vessels. The tiny blood vessels that nourish the retina are damaged by the increased glucose level. Diabetes is the fifth-deadliest disease in the USA, and still there is no cure. The total annual economic cost of diabetes in 2002 was estimated to be US $132 billion, or one out of every 10 health care dollars spent in the USA [**1**].

*Corresponding author: Department of Electronics and Computer Engineering, Ngee Ann Polytechnic, 535 Clementi Road, Singapore, 599489, Singapore.
email: aru@np.edu.sg; acharyaur@yahoo.com

Diabetic retinopathy (DR) occurs when diabetes damages the tiny blood vessels inside the retina, the light-sensitive tissue at the back of the eye [**2**]. This tiny blood vessel will leak blood and fluid on the retina, forming features such as microaneurysms, haemorrhages, hard exudates, cotton wool spots, or venous loops [**2**, **3**]. DR can be broadly classified as non-proliferative diabetic retinopathy (NPDR) and proliferative diabetic retinopathy (PDR) [**3**]. Depending on the presence of features on the retina, the stages of DR can be identified [**3**].

DR has four stages [**3**, **4**].

1. *Mild non-proliferative retinopathy*. At least one microaneurysm with or without the presence of retinal haemorrhages, hard exudates, cotton wool

spots, or venous loops will be present. Approximately 40 per cent of people with diabetes have at least mild signs of DR [**5**].

2. *Moderate non-proliferative retinopathy.* Numerous microaneurysms and retinal haemorrhages will be present. Cotton wool spots and a limited amount of venous beading can also be seen. 16 per cent of the patients with moderate NPDR will develop PDR within 1 year [**6**].
3. *Severe non-proliferative retinopathy.* This is characterized by any one of the following (4–2–1 rule) characteristics:
   (a) numerous haemorrhages and microaneurysms in four quadrants of the retina;
   (b) venous beading in two or more quadrants;
   (c) intraretinal microvascular abnormalities in at least one quadrant;
   (d) severe NPDR carries a 50 per cent chance of progression to PDR in 1 year. Patients with two or more of these features are graded as very severe NPDR [**6**].
4. *Proliferative retinopathy.* This is the advanced stage; the signals sent by the retina for nourishment trigger the growth of new blood vessels. These new blood vessels are abnormal and fragile. They grow along the retina and along the surface of vitreous gel which fills inside the eye. These blood vessels do not cause symptoms or vision loss, but their walls are thin and fragile. It may result in severe vision loss and even blindness, if they leak the blood. About 3 per cent of people in this condition may suffer severe visual loss [**5**].

The algorithm for the automatic detection of the exudates and the haemorrhage and microaneurysms (HMAs) was developed using recursive region growing segmentation combined with the moat operator [**7**]. It was able to identify exudates with a sensitivity and a specificity of 88.5 per cent and 99.7 per cent respectively and HMAs with a sensitivity and a specificity of 77.5 per cent and 88.7 per cent respectively. Various statistical classifiers, namely Bayesian, Mahalanobis, and *k*-nearest neighbour classifiers were tested for the detection of the salient features of the DR images [**8**]. The Mahalanobis classifier showed the best result for the statistical classifiers in detecting microaneurysms, haemorrhages, exudates, and cotton wool spots with sensitivities of 69 per cent, 83 per cent, 99 per cent, and 80 per cent, respectively.

A multi-resolution segmentation vessel tracker algorithm was developed to detect the optical disc, bright lesions (cotton wool spots), and dark lesions (haemorrhages) [**9**]. This algorithm identifies the veins and arteries with accuracies of 78.4 per cent and 66.5 per cent respectively. Automatic detection of the exudates was proposed using coarse segmentation by fuzzy *C*-means clustering and fine segmentation by morphological reconstruction [**10**]. The sensitivity and specificity of the detection of these exudates were 86 per cent and 99 per cent respectively.

Many algorithms and techniques have been developed to extract different features from the fundus images [**11**, **12**]. Colour features in the Bayesian statistical classifier was used to classify each pixel into lesion or non-lesion classes [**13**]. Experimental results indicate that they were able to achieve 100 per cent accuracy in identifying all the retinal images with exudates, while maintaining 70 per cent accuracy in correctly classifying the truly normal retinal images as 'normal'.

In recent years, several researchers have developed systems for automatic identification of features for DR, which were useful in therapeutic treatment [**14**–**17**]. These are useful in subjective analysis of the disease and specific features of the disease, but they do not provide any methods for automatic detection of different stages of the disease.

Researchers have used the areas and perimeter of the red–green–blue (RGB) components of the blood vessels to classify normal, moderate DR, severe DR, and prolific DR stages with an accuracy of 84 per cent [**18**] and normal, mild DR, moderate to severe DR, and PDR with an accuracy of 77 per cent [**3**]. Nayak *et al.* [**4**] have classified the fundus images into normal, NPDR, and PDR classes with an accuracy of 93 per cent. Recently, higher-order spectra features were used as input to the support vector machine (SVM) classifier to classify the images into normal, mild DR, moderate DR, severe DR, and PDR classes with an accuracy of 82 per cent [**19**]. A software to grade the severity of three types of early lesion, namely, haemorrhages and microaneurysms, hard exudates, and cotton wool spots, of DR was proposed to classify NPDR [**20**]. They were able to identify with accuracies of 82.6 per cent, 82.6 per cent, and 88.3 per cent using the 430 images and of 85.3 per cent, 87.5 per cent, and 93.1 per cent using the 361 images respectively, for haemorrhages and microaneurysms, hard exudates, and cotton wool spots.

In this paper, four salient features, namely the area of blood vessels, microaneurysms, exudates, and haemorrhages, have been extracted and classified into five classes using the SVM classifier. Figure 1

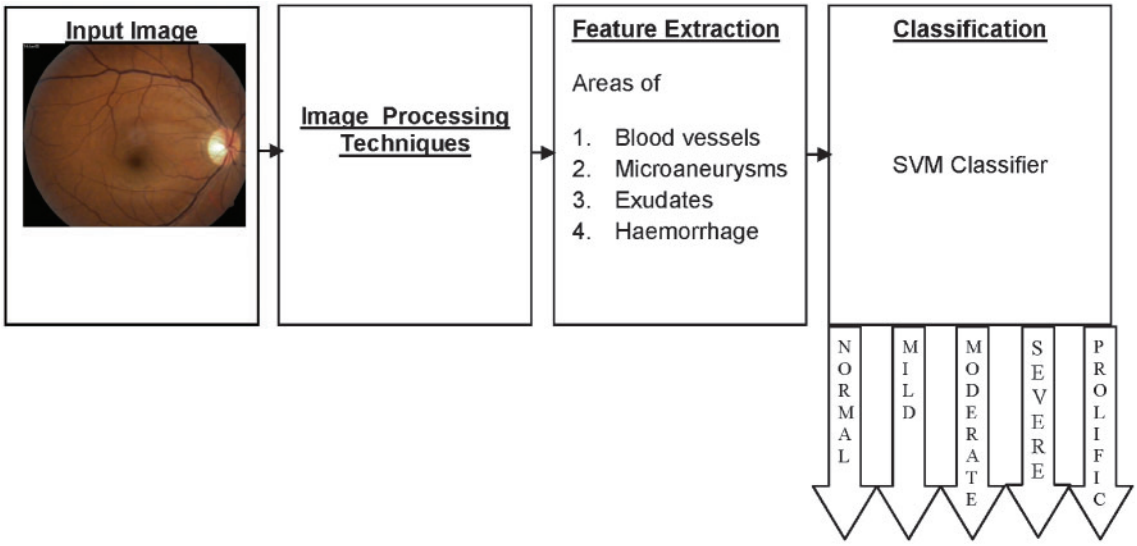

Fig. 1 Proposed system for the detection and classification of different stages of DR

shows the proposed system for identification of DR stages.

2 COMPUTER METHODS AND THEORY

In this work, 331 retinal photographs of moderate NPDR, severe NPDR, PDR, and also normal cases, have been studied. These data were provided by the National University Hospital, Singapore. The number and details of photographs in each group are shown in Table 1. Images taken with a Ziess Visucam^{lite} fundus camera interfaced to a computer, were stored in 24 bit JPEG format with an image size of 256×256 pixels.

2.1 Feature extraction

Features, namely areas of blood vessels, microaneurysms, exudates, and haemorrhages, were extracted from the fundus image. A brief description of these features is given below.

2.1.1 Detection of blood vessels

The detection of blood vessels is one of the very important features in the identification of DR stages.

Table 1 Ranges of age and number of subjects in each group

Type	Age (years)	Number of subjects
Normal	32 ± 8	62
Mild DR	48 ± 14	73
Moderate DR	58 ± 13	65
Severe DR	45 ± 12	71
PDR	70 ± 10	60

In the present work, morphological image-processing techniques were used to detect the blood vessels. The green channel of the fundus RGB image was used for obtaining the traces of blood vessels [**21**].

First the image intensity levels were inverted. Adaptive histogram equalization was performed to improve the contrast of the image. A morphological 'opening' operation was conducted using the 'ball' structuring element to smooth the background and to highlight the blood vessels of the image [**22**]. Each image was subtracted from the equalized image. This resulting image shows higher intensity values at the blood vessels compared with the background. Then the image was binarized by the thresholding method. Median filtering was conducted on this binarized image to remove the noise. A border was created around the image for extracting blood vessels. Then the remaining noise within the image was eliminated. The intensity values of image with only borders were subtracted from the inverted intensity values of this image to eliminate the edges. Then the pixel values of the images are inverted to obtain the final image with only blood vessels. Figure 2 shows the result of the blood vessel detection for normal, mild DR, moderate DR, severe DR, and PDR.

2.1.2 Detection of exudates

The green component of the RGB image is used to identify the exudates too [**4**, **21**]. Two structuring elements (SEs), namely octagon-shaped SEs and disc-shaped SEs, were used. A morphological closing

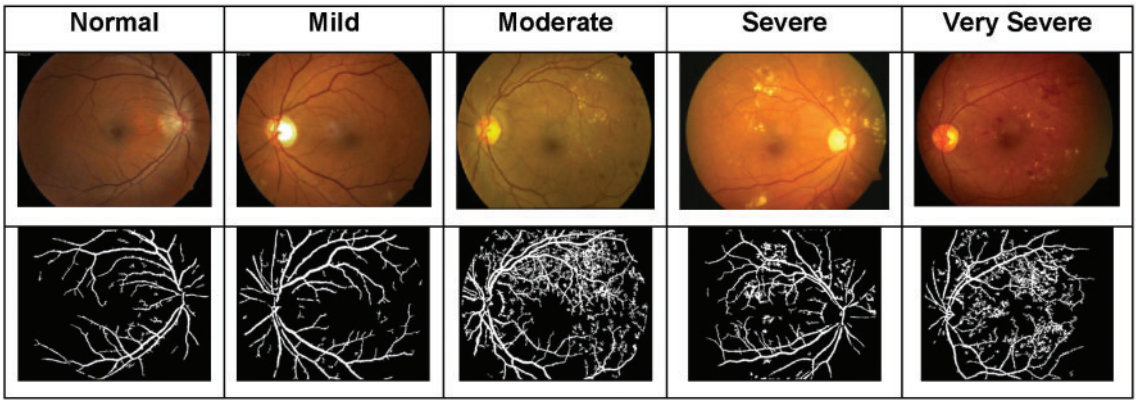

Fig. 2 Results of the detection of blood vessels for normal, mild DR, moderate DR, severe DR, and PDR stages

operation was performed using an octagon-shaped SE. This results in a good contrast image between the exudates and the background [**22**]. However, the optical disc will also be present together with the exudates, as their grey levels are comparable with those of exudates.

Columnwise neighbourhood operation was performed to remove the unwanted background artefacts, leaving only the exudates and the optical disc. Exudates have irregular shapes and borders. To solve this problem, morphological closing with a disc-shaped SE was used. After determining the proper threshold, exudates were obtained. The optical disc usually occupies approximately one seventh of the entire image, 80×80 pixels, and is the part of the retina which has the highest pixel value. A region of interest was then specified to remove the optical disc.

Finally, by performing an opening operation using a disc-shaped SE, exudates were extracted. Figure 3 shows the result of the exudates detection of normal, mild DR, moderate DR, severe DR, and PDR.

2.1.3 Detection of microaneurysms

The green component of the RGB image was used to identify the microaneurysms [**23**]. First the pixel intensities of the image were inverted. In order to eliminate the borders of the images, the edge-detected image (using Canny's method) was subtracted from the image with only the border [**22**]. This results in an edge-detected image with microaneurysms and its gaps are filled. The original image (without filling of the gaps) was subtracted from this image (after filling the gaps). The resulting image thus has microaneurysms and unwanted filled gaps also.

The blood vessels were detected using the above method (section 2.1.1). Then the image was subjected to edge detection using Canny's method.

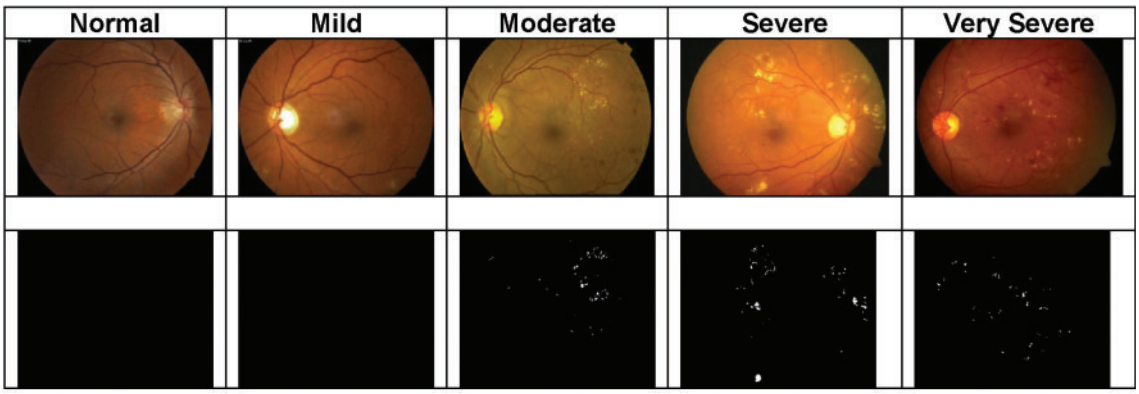

Fig. 3 Results of the detection of exudates for normal, mild DR, moderate DR, severe DR, and PDR stages

Then, this image was subtracted from the above edge-detected image with microaneurysms. This results in an image with distorted blood vessels. After filling the gaps, this image was subtracted from the above image with microaneurysms and artefacts. Now, the resulting image will have only microaneurysms. Figure 4 shows the result of the detection of microaneurysms for normal, mild DR, moderate DR, severe DR, and PDR.

2.1.4 Detection of haemorrhages

There are two parts in the detection of haemorrhages:

(a) detection of blood vessels;
(b) detection of blood vessels with haemorrhages.

The haemorrhages are of the same intensity as the blood vessels. Hence, it is difficult to perform any processing on the image to reveal only the haemorrhages. The only way to extract the haemorrhages is to subtract the blood vessels from blood vessels with haemorrhages. The pixel intensity values of the red channel of the RGB image are inverted and is subjected to adaptive histogram equalization [**22**]. 'Ball'-shaped SEs of sizes 6 and 25 are chosen to identify the blood vessels and blood vessels with haemorrhages. These two sizes of SE were chosen by the trial-and-error method. Brief details of the method are given below.

Detection of blood vessels alone. The image was subjected to erosion and dilation using a 'ball'-shaped SE of size 6. It helps in the detection of blood vessels alone. The resulting image intensity was enhanced. Then the image is dilated and subtracted from the enhanced image. The resulting image is again enhanced to obtain the blood vessels alone.

Detection of blood vessels with haemorrhages. The image was subjected to erosion and dilation using a 'ball'-shaped SE of size 25. The use of a large SE is essential to the blood vessels with haemorrhages. The resulting image intensity is enhanced. Then the image is dilated and subtracted from the enhanced image. The resulting image is again enhanced to obtain the blood vessels and haemorrhages.

Now, the image with blood vessels alone was subtracted from the image with blood vessels and haemorrhages to obtain the image with haemorrhages and artefacts. Median and Wiener filtering were performed to eliminate unwanted artefacts in the image after thresholding. After removing the optical disc from this image, the resulting image will have only haemorrhages. Figure 5 shows the result of the detection of haemorrhages for normal, mild DR, moderate DR, severe DR, and PDR.

3 CLASSIFIER USED

In this study a SVM classifier was used for the identification of the different classes of DR. A brief description of the SVM is given below.

3.1 Support vector machine

In recent years, SVM classifiers have demonstrated excellent performance in a variety of pattern recognition problems [**16**, **24**, **25**]. SVMs were initially designed for the two-class problems but subsequently extended to multi-class problems. A brief description of the two-class approach is given below.

The SVM searches for a hyperplane as a decision surface which separates positive and negative examples from each other with the maximum margin. This involves orienting the separating hyperplane to

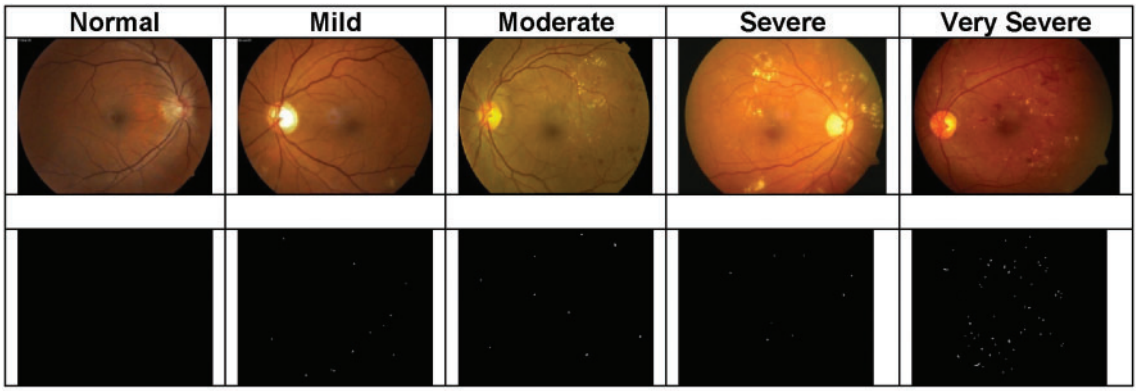

Fig. 4 Results of the detection of microaneurysms for normal, mild DR, moderate DR, severe DR, and PDR stages

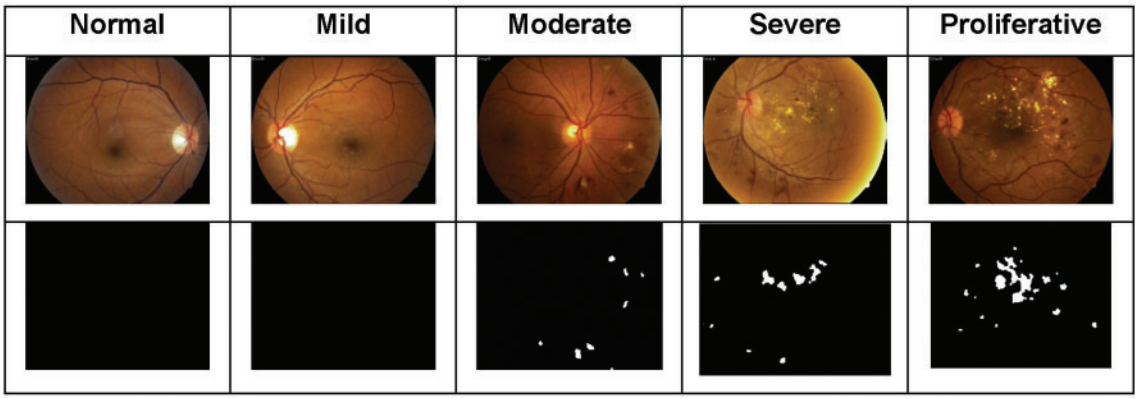

Fig. 5 Results of the detection of haemorrhages for normal, mild DR, moderate DR, severe DR, and PDR stages

be perpendicular to the shortest line separating the convex hulls of the training data for each class, and locating it midway along this line.

Let the separating hyperplane be defined by $\boldsymbol{x}$, $\boldsymbol{w}+b=0$, where $\boldsymbol{w}$ is its normal. For linearly separable data labelled $\{\boldsymbol{x}_i, \boldsymbol{y}_i\}$, $\boldsymbol{x}_i \in \Re^n$, $y_i = \{-1, 1\}$, $i = 1, 2, \ldots, N$ the optimum boundary chosen with maximum margin criterion can be found by minimizing the objective function

$$E = \|\boldsymbol{w}\|^2 \quad \text{subject to} (\boldsymbol{x}_i \cdot \boldsymbol{w} + b) y_i \geqslant 1, \text{ for all } i \tag{1}$$

The solution for the optimum boundary $\boldsymbol{W}_0$ is a linear combination of the training data $\boldsymbol{s}$ $\{1, \ldots, N\}$, the *support vectors*. This solution can be obtained easily by translating it into its 'dual form'. The optimization problem can then be solved with quadratic programming methods [**24**, **26**], giving the optimum decision boundary $\boldsymbol{W}_0$ as

$$\boldsymbol{W}_0 = \sum_i \alpha_i y_i \boldsymbol{x}_i \tag{2}$$

which is a linear combination of the support vectors with $\alpha_i \neq 0$.

Kernel functions can be used to extend the solution to non-linear boundary problems [**27**]. The dot product in the feature space is expressed by the kernels of two vectors in input space. The polynomial and radial basis function (RBF) kernels are commonly used [**26**].

Several algorithms are available to extend the basic binary SVM classifier to the multi-class classifier. They may be as follows:

(a) one-against-one SVM;
(b) one-against-all SVM [**28**];
(c) half-against-half SVM [**29**];
(d) directed acyclic graph (DAG) SVM [**30**]. In this work, the RBF kernel function was used with a one-against-all algorithm to classify input features. An initial search was performed for the parameters for the SVM by using a 'grid search' approach [**31**]. 240 images were used for training and 91 images for testing.

4 RESULTS

The features were analysed using the p value obtained using an analysis of variance (ANOVA) between groups. ANOVA uses variances to decide whether the *means* are different. In the present study, this test was used to compute the variation between features within a class and between classes. When the variation between classes was seen to be relatively high compared with the variation within the class, the test was considered to be statistically significant (low value of p).

Table 2 shows the range of the four extracted features. In this study, more blood vessels were observed in the normal images. The exudates, haemorrhages, and microaneurysms were absent in the case of the normal fundus image. In the case of mild DR and moderate DR, all the four features were present. Exudates were more predominant in the case of severe DR and haemorrhages in PDR. All the four features are clinically significant ($p < 0.0001$).

Table 3 shows the results of the present classification using the SVM. The results indicate that the classifier is effective to about 85 per cent in making the correct prediction of the unknown class. It is able to predict correctly moderate DR, mild DR, severe DR, and PDR up to 94 per cent, 80 per cent, 85 per

Table 2 Ranges of input features to the classifier

Feature	Mean ± standard deviation					p value
	Normal	Mild DR	Moderate DR	Severe DR	PDR	
Blood vessels	70 648 ± 32 160	58 207 ± 26 600	60 413 ± 30 280	34 629 ± 24 680	35 754 ± 29 890	< 0 .0001
Exudates	7.5 ± 16.8	234.79 ± 444	653.02 ± 872	796.72 ± 1006	842.98 ± 1169	< 0.0001
Haemorrhages	829.47 ± 1292	5792.1 ± 7473	4155.87 ± 6042	11 620 ± 8099	8972.3 ± 8293	< 0.0001
Microaneurysms	53.774 ± 61.8	165.66 ± 151	241.48 ± 153	236.28 ± 203	281.43 ± 277	< 0.0001

Table 3 Training and testing data sets

Class	Number of data sets used for training	Number of data sets used for testing	Percentage (%) of correct classifications
Normal	45	17	82.35
Mild DR	53	20	80
Moderate DR	48	17	94.11
Severe DR	51	20	85
PDR	43	17	88.24
Average			85.94

cent, and 88.24 per cent respectively. The classifier showed a sensitivity of 82 per cent, a specificity of 86 per cent, and a positive predictive value of 95 per cent (Table 4).

5 DISCUSSION

The important features of the fundus images, namely exudates, haemorrhages, and microaneurysms, were extracted (Table 5) and software was developed for the computer-based screening of the DR subjects [**32**]. This program was able to differentiate DR class from the normal subjects correctly with a sensitivity of 74 per cent and a specificity of 82.7 per cent.

DR was differentiated from a normal retina using image-processing algorithms by Sinthanayothin *et al.* [**7**]. In their method, retinal images were preprocessed using adaptive local contrast enhancement. Their system, based on a multi-layer perceptron neural network, yielded a sensitivity of 80.21 per cent and a specificity of 70.66 per cent.

A decision support system for the early detection of the DR (presence of the microaneurysms) was proposed by Kahai *et al.* [**33**]. The detection rule is based on a binary-hypothesis testing problem with yes–no decisions. The Bayes optimality criterion was applied to fundus images for the early detection of the DR. This system was able to identify the presence of microaneurysms with a sensitivity of 100 per cent and specificity of 67 per cent accurately.

Table 4 Sensitivity, specificity, and positive predictive accuracy of the SVM classifier

Classifier	TN	TP	FP	FN	Sensitivity (%)	Specificity (%)	Positive predictive accuracy (%)
SVM	14	64	3	10	82.35	86.49	95.5

Table 5 Automatic detection of the DR stages by various researchers

Number	Reference	Number of classes	Method	Accuracy of classification (%)	Sensitivity (%)	Specificity (%)
1	Sinthanayothin *et al.* [**7**]	2	Moat operator	Not reported	80.21	70.66
2	Singalavanija *et al.* [**32**]	2	Blood vessels, exudates, haemorrhages, and microaneurysms	Not reported	74.8	82.7
3	Kahai *et al.* [**33**]	2	Decision support system	Not reported	100	63
4	Wong *et al.* [**18**]	4	Area of blood vessels	84	91.7	100
5	Nayak *et al.* [**4**]	3	Blood vessels, exudates, and texture	93.6	90.3	100
6	Acharya *et al.* [**14**]	5	Higher order spectra	82	82.5	88.9
7	This work	5	Blood vessels, exudates, microaneurysms, and haemorrhages	85.9	82	86

Wong *et al.* [**18**] have classified normal, mild DR, moderate DR, severe DR, and PDR stages using morphological image-processing techniques and a feedforward neural network [**18**]. In their work, the area and perimeter of the RGB components of the blood vessels are chosen as the features for the classifier. The average classification efficiency of their system was 84 per cent, the sensitivity was 90 per cent, and the specificity was 100 per cent. Using the area of the exudates, blood vessels, and texture parameters, the fundus images were classified into normal, NPDR, and PDR [**4**]. They demonstrated a classification accuracy of 93 per cent, a sensitivity of 90 per cent, and a specificity of 100 per cent.

Recently, Acharya *et al.* [**19**] automatically identified normal, mild DR, moderate DR, severe DR, and PDR stages using the bispectral invariant features of higher-order spectra techniques and a SVM classifier [**19**]. They obtained an average accuracy of 82 per cent in identifying the unknown class, a sensitivity of 82 per cent, and a specificity of 88 per cent.

In the present work, the DR classes are classified into five classes using haemorrhages, microaneurysms, exudates, and blood vessel areas. A SVM was used for the automatic identification. The classifier is able to identify the unknown class accurately with an efficiency of more than 85 per cent. The images of the diabetes stages were provided by ophthalmologists after their diagnosis using traditional indirect retinal microscopy. The diagnosis of the unknown DR class matches the diagnosis of the ophthalmologists to more than 85 per cent.

The sensitivity and specificity of the system are 82 per cent and 85 per cent respectively and will help in the screening of retina for diabetes patients at least once a year. However, it may not be possible to substitute the present results for the traditional retinal examination; however, the accuracy of the system can be further increased by adding more features such as the distance of the exudates from the fovea and the texture. Also, when more diverse DR images are taken under identical lighting conditions and orientations, this may improve the results in diagnosing the correct class of the unknown input image. The software for the extraction of the features using image processing and identification of the different classes was written in MATLAB 7.0.4.

6 CONCLUSION

An optometrist uses an ophthalmoscope that sends light and magnifies the blood vessels to detect the DR stages. In the present work, an automated technique was proposed to identify the DR stages using simple image-processing and data-mining techniques. The system can identify different stages with an average accuracy of more than 85 per cent, a sensitivity of 82 per cent, and a specificity of 86 per cent. The performance can be further increased with more diverse data and better features.

ACKNOWLEDGEMENTS

The present authors thank Ms Gracielynne Flores Encio and Ms Melissa Tan Yan Jun for their contribution in the development of the software.

REFERENCES

1 Diabetes and retinopathy (eye complications), available from http://www.diabetes.org/diabetes-statistics/eye-complications.jsp (accessed 3 January 2008).
2 **Frank, R. N.** Diabetic retinopathy. *Prog. Retinal Eye Res.*, 1995, **14**(2), 361–392.
3 **Acharya, U. R., Ng, E. Y. K.,** and **Suri, J. S.** *Image modelling of human eye*, 2008 (Artech House, Norwood, Massachusetts).
4 **Nayak, J., Bhat, P. S., Acharya, U. R., Lim, C. M.,** and **Kagathi, M.** Automated identification of different stages of diabetic retinopathy using digital fundus images. *J. Med. Systems*, 2008, **32**(2), 107–115.
5 Diabetic 'retinopathy', available from http://www.hoptechno.com/book45.htm (accessed 17 January 2008).
6 International Council of Ophthalmology, International Standards, International clinical diabetic retinopathy disease severity scale, detailed table, October 2002, available from http://www.icoph.org/standards/pdrdetail.html.
7 **Sinthanayothin, S., Boyce, J. F., Williamson, T. H.,** and **Cook, H. L.** Automated detection of diabetic retinopathy on digital fundus image. *Int. J. Diabetic Medicine*, 2002, **19**, 105–112.
8 **Ege, B. M., Hejlesen, O. K., Larsen, O. V., Møller, K., Jennings, B., Kerr, D.,** and **Cavan, D. A.** Screening for diabetic retinopathy using computer based image analysis and statistical classification. *Computer Methods Programs Biomedicine*, 2000, **62**(3), 165–175.
9 **Englmeier, K. H., Schmid, K., Hildebrand, C., Bichler, S., Porta, M., Maurino, M.,** and **Bek, T.** Early detection of diabetes retinopathy by new algorithms for automatic recognition of vascular changes. *Eur. J. Med. Res.*, 2004, **9**(10), 473–488.
10 **Sopharak, A.** and **Uyyanonvara, B.** Automatic exudates detection from diabetic retinopathy retinal image using fuzzy *c*-means and morphological methods. In Proceedings of the Third IASTED

International Conference on *Advances in computer science and technology (ACST 2007)*, Phuket, Thailand, 2–4 April 2007, pp. 359–364 (Acta Press, Calgary, Alberta).

11 **Osareh, A., Mirmehdi, M., Thomas, B.,** and **Markham, R.** Comparative exudate classification using support vector machines and neural networks. In Proceedings of the Fifth International Conference on *Medical image computing and computer-assisted intervention (MICCAI 2002)*, Lecture Notes in Computer Science, vol. 2489, Tokyo, Japan, 25–28 September 2002, pp. 413–420 (Springer-Verlag, Berlin).

12 **Walter, T., Klein, J.-C., Massin, P.,** and **Erginay, A.** A contribution of image processing to the diagnosis of diabetic retinopathy – detection of exudates in color fundus images of the human retina. *IEEE Trans. Med. Imaging*, 2002, **21**(10), 1236–1243.

13 **Wang, H., Hsu, W., Goh, K. G.,** and **Lee.** An effective approach to detect lesions in color retinal images. In Proceedings of the IEEE Conference on *Computer vision and pattern recognition*, 2000, vol. 2, pp. 181–186 (IEEE, New York).

14 **Kandiraju, N., Dua, S.,** and **Thompson, H. W.** Design and implementation of a unique blood vessel detection algorithm towards early diagnosis of diabetic retinopathy. In Proceedings of the International Conference on *Information technology: coding and computing* (ITCC'05), 2005, pp. 26–31 (IEEE Computer Society, New York).

15 **Larsen, M., Godt, J., Larsen, N., Lund-Andersen, H., Sjolie, A. K., Agardh, E., Kalm, H., Grunkin, M.,** and **Owens, D. R.** Automated detection of fundus photographic red lesions in diabetic retinopathy. *Invest. Ophthalmology Visual Sci.*, 2003, **44**(2), 761–766.

16 **Vapnik, V.** *Statistical learning theory*, 1998 (John Wiley, New York).

17 **Xiaohui, Z.** and **Chutatape, A.** Detection and classification of bright lesions in color fundus images. In Proceedings of the International Conference on *Image processing (ICIP 04)*, 2004, vol. 1, pp. 139–142 (IEEE, New York).

18 **Wong, L. Y., Acharya, U. R., Venkatesh, Y. V., Chee, C., Lim, C. M.,** and **Ng, E. Y. K.** Identification of different stages of diabetic retinopathy using retinal optical images. *Inf. Sci.*, 2008, **178**(1), 106–121.

19 **Acharya, U. R., Chua, K. C., Ng, E. Y. K., Wei, W.,** and **Chee, C.** Application of higher order spectra for the identification of diabetes retinopathy stages. *J. Med. Systems*, 2008, **32**(6), 481–488.

20 **Lee, S. C., Lee, E. T., Wang, Y., Klein, R., Kingsley, R. M.,** and **Warn, A.** Computer classification of nonproliferative diabetic retinopathy. *Arch Ophthalmology*, 2005, **123**(6), 759–764.

21 **Li, H.** and **Chutatape, O.** Fundus image feature extraction. In Proceedings of the 22nd Annual International Conference of the IEEE Engineering on Medicine and Biology Society, Chicago, Illinois, USA, 23–28 July 2000, pp. 3071–3073 (IEEE, New York).

22 **Gonzalez, R. C.** and **Wintz, P.** *Digital image processing*, 2nd edition, 1987 (Addison-Wesley, Reading, Massachusetts).

23 **Walter, T., Massin, P., Erginay, A., Ordonez, R., Jeulin, C.,** and **Klein, J. C.** Automatic detection of microaneurysms in color fundus images. *Med. Image Analysis*, 2007, **11**(6), 555–566.

24 **Burgess, C. J.** A tutorial on support vector machines for pattern recognition. *Data Mining Knowledge Discovery*, 1998, **2**(2), 1–47.

25 **Shon, T.** and **Moon, J.** A hybrid machine learning approach to network anomaly detection. *Inf. Sci.*, 2007, **177**(18), 3799–3821.

26 **Christianini, N.** and **Taylor, J.** *Support vector machines and other kernel-based learning methods*, 2000 (Cambridge University Press, Cambridge).

27 **Muller, K. R., Mika, S., Ratsch, G., Tsuda, K.,** and **Scholkopf, B.** An introduction to kernel based learning algorithms. *IEEE Trans. Neural Networks*, 2001, **12**(2), 181–201.

28 **Lingras, P.** and **Butz, C.** Rough set based 1–v–1 and 1–v–r approaches to support vector machine multi-classification. *Inf. Sci.*, 2007, **177**(18), 3782–3798.

29 **Lei, H.** and **Govindaraju, V.** Half-against-half multi-class support vector machines. In Proceedings of the Sixth International Workshop on *Multiple classifier systems (MCS 05)*, 2005, pp. 156–164 (Springer-Verlag, Berlin).

30 **Platt, C. J., N. Chrisianini, N.,** and **Shawe-Taylor, J.** Large Margin DAGs for multiclass classification. *Adv. Neural Inf. Processing Systems*, 200, **12**, 547–553.

31 **Hsu, C. W., Chang, C. C.,** and **Lin, C. J.** A practical guide to support vector classification. Technical report, Department of Computer Science, National Taiwan University, Taiwan, Republic of China, 2003.

32 **Singalavanija, A., Supokavej, J., Bamroongsuk, P., Sinthanayothin, C., Phoojaruenchanachai, S.,** and **Kongbunkiat, V.** Feasibility study on computer-aided screening for diabetic retinopathy. *Jap. J. Ophthalmology*, 2006, **50**(4), 361–366.

33 **Kahai, P., Namuduri, K. R.,** and **Thompson, H.** A decision support framework for automated screening of diabetic retinopathy. *Int. J. Biomed. Imaging*, 2006, 1–8.